Deficient CCR7 signaling promotes T_H2 polarization and B-cell activation

in vivo



 $G.\ Leandros\ Moschovakis^1,\ Anja\ Bubke^1,\ Oliver\ Dittrich-Breiholz^2,\ Asolina\ Braun^1,\ Immo$

Prinz¹, Elisabeth Kremmer³ and Reinhold Förster¹

¹Institute of Immunology, Hannover Medical School, D-30625 Hannover, Germany;

²Institute for Physiological Chemistry, Hannover Medical School, D-30625 Hannover,

Germany;

³Institute of Molecular Immunology, Helmholtz Zentrum München, D-81377 Munich,

Germany

CCR7 modulates T-cell differentiation

Corresponding author:

Prof. Dr. Reinhold Förster, Institute of Immunology, Hannover Medical School, Carl-

Neuberg-Strasse 1, D-30625 Hannover, Germany;

e-mail: foerster.reinhold@mh-hannover.de

Abbreviations used in this paper: pLNs, peripheral lymph nodes; SLOs, secondary

lymphoid organs; FMO, fluorescence-minus-one;

© 2011 WILEY-VCH Verlag GmbH & Co. KGaA, Weinheim

Received: May 13, 2011 / Revised: August 16, 2011 / Accepted: September 27, 2011

DOI: 10.1002/eji.201141753

Summary

Immuno

The chemokine receptor CCR7 has a central role in regulating homing and positioning of T cells and DCs to lymph nodes and participates in T-cell development and activation. In this study we addressed the role of CCR7 signaling in T_H2 polarization and B-cell activation. We provide evidence that lack of CCR7 drives the capacity of naïve CD4⁺ T cells to polarize towards T_H2 cells. This propensity contributes to a lymph node environment in CCR7-deficent mice characterized by increased expression of IL-4 and increased frequency of T_H2 cells. We show that elevated IL-4 levels lead to B-cell activation characterized by upregulated expression of MHC class II, CD23 and CD86. Activated B cells are in turn highly efficient in presenting antigen to CD4⁺ T cells and thus potentially contribute to the T_H2 microenvironment. Taken together, our results support the idea of a CCR7-dependent patterning of T_H2 responses, with absent CCR7 signaling favoring T_H2 polarization, dislocation of T helper cells into the B-cell follicles and, as a consequence, B-cell activation.

1. Introduction

The chemokine receptor CCR7 is expressed on several cells of the immune system including mature dendritic cells (DCs), activated plasmacytoid DC (pDCs), naïve and central memory T cells, as well as B cells [1-4]. The ligands for CCR7, the chemokines CCL19 and CCL21, are homeostatically expressed in lymphoid organs as well as in terminal lymphatic vessels and play an important role in the homing of DCs and lymphocytes to secondary lymphoid organs (SLOs) and their positioning within defined compartments therein [5]. CCR7^{-/-} mice display a severely altered micro-architecture in SLOs reflecting the profound defects of T-cell and DC homing [6]. Surprisingly, CCR7^{-/-} mice are not immunodeficient in a strict sense as they have been reported to display exacerbated contact hypersensitivity responses to oxazolone and enhanced immune reactions after immunization with tetanus toxoid [7]. Furthermore, CCR7^{-/-} mice are able to elicit a robust antiviral B-cell response following VSV infection leading to similar VSV-specific Ig titers in wild-type and CCR7^{-/-} mice [8]. CCR7^{-/-} mice also display elevated serum titers of IgG to dsDNA in serum and IgG deposits in renal glomeruli, reflecting their high propensity to develop autoimmunity [9]. B cells are present in regular numbers in LNs of CCR7^{-/-} mice, but these cells display several deviations from the phenotype of wild-type cells. B cells isolated from the peripheral lymph nodes (pLNs) of CCR7^{-/-} mice express increased levels of surface MHC class II (MHC-II), and IgD⁻ IgM^{low} B cells are present at higher frequencies. Furthermore, altered isotype switching is observed in CCR7^{-/-} mice [6]. It is currently unclear whether this altered B-cell phenotype is a consequence of an inherent B-cell defect or whether it is due to the altered microenvironment in LNs of CCR7^{-/-} mice, reflecting possibly aberrant cell-cell interactions and/or altered secretion of soluble factors. Moreover, in addition to the well established role of CCR7 as a homing receptor directing the migration of cells into SLOs, increasing evidence suggests that CCR7-mediated signals contribute to other cellular processes such as modulation of cell proliferation, activation or differentiation [10-12].

In the present study we reveal the mechanisms that cause B-cell activation in the non-inflamed LNs in CCR7^{-/-} mice. Applying adoptive cell transfers we show that factors within the LN environment determine the level of B-cell activation irrespective of their CCR7 expression. With RT-PCR and in vivo neutralization experiments we provide evidence that IL-4 is over-expressed in pLNs of CCR7^{-/-} mice and significantly contributes to the activation of B cells. Furthermore, we demonstrate that upon T-cell stimulation and T_H2 polarization, CCR7^{-/-} CD4⁺ T cells differentiate with higher frequency to IL-4-secreting cells than CCR7^{+/+} CD4⁺ T cells. Taken together, we provide evidence that deficient CCR7 signaling fosters a T_H2 environment in LNs with increased IL-4 secretion from CD4⁺ T cells and activation of B cells. These results reveal new aspects of CCR7 function in the homeostasis of the immune system, complementing its known role in cell migration.

2. Results

B cells in pLNs of CCR7^{-/-} mice are activated

In order to identify the mechanisms underlying increased surface MHC-II levels on B cells we described earlier in CCR7^{-/-} mice [6] the expression of cell surface levels of MHC-II, as well as other activation markers such as CD86, and the low-affinity Fce receptor (CD23) was analyzed. Compared with Balb/c mice B cells residing in pLNs of CCR7^{-/-} mice display an activated phenotype with significantly increased expression of MHC-II, CD86 and CD23 (Fig. 1A). Semi-quantitative analysis revealed an approximately 2.5 fold increase in MHC-II and CD86 while CD23 was approximately 2-fold up-regulated. While in CCR7^{-/-} mice CD23 was also up-regulated on blood and splenic B cells, we failed to observe any difference between the two genotypes regarding MHC-II or CD86 expression on B cells isolated from spleen or blood (Fig. 1B). Similar results were obtained with CCR7^{-/-} mice on the C57BL/6 genetic background (Fig. S1). To test the idea that up-regulation of these markers is caused by a potentially increased pathogenic load in CCR7^{-/-} mice we also analyzed wild type and CCR7^{-/-} mice kept under germ-free conditions. Up-regulation of MHC-II and CD86 was also observed on B cells in CCR7^{-/-} mice kept under germ-free conditions, suggesting that intrinsic - rather than microbial factors are responsible for B-cell activation in CCR7^{-/-} mice (Fig. S2). We found a similarly altered activation status of B cells in *plt/plt* mice (Fig. S1), which carry a spontaneous genetic deletion that prevents the expression of the CCR7 ligands, CCL19 and CCL21 in secondary lymphoid organs [13], suggesting that absence of signaling through CCR7 and not merely CCR7 deficiency is responsible for the altered B-cell phenotype.

To delineate further effects of CCR7 deficiency on gene expression in B cells, highly purified CD19⁺ cells from pLNs of CCR7^{-/-} mice or wild-type controls were sorted and subjected to whole mouse genome microarray analysis (GEO accession: GSE27885). Very few genes were differentially regulated in CCR7^{-/-} B cells and the differences in mRNA expression were only minor. Out of the 15547 functionally annotated mRNA transcripts

regulated in CCR7^{-/-}B cells in each of two experiments performed (Table S1). Genes with deregulated expression and being known for having a role in B-cell activation are presented in Fig. 1C. The expression of Immunoglobulin joining chain (Igj), Activation-induced cytidine deaminase (Aicda), Secretory leukoprotease inhibitor (Slpi), Nuclear factor, IL-3-regulated (Nfil3) and SAM domain, SH3 domain and nuclear localization signals, 1 (Samsn1) was upregulated 4.8-, 3.3-, 3.1-, 3.1-, and 2.7-fold, respectively, in CCR7^{-/-} B cells. For all these genes increased transcripts upon B-cell activation have been reported, especially in response to IL-4 as regards Aicda, Nfil3 and Samsn1 [14-18]. mRNA expression levels of Krüppel-like factor 4 (Klf4) and regulators of G-protein signaling 1 and 2 (Rgs1, Rgs2) were downregulated 2.5-, 4.6-, and 2.9-fold, respectively, in CCR7^{-/-} B cells. *KLf4* expression has been reported to increase during B-cell maturation and to decrease upon B-cell activation [19]. Rgs1 and Rgs2 down-regulate chemotaxis to lymphoid chemokines and their expression levels were shown to vary considerably depending on the B-cell activation regimen applied [20]. Genes encoding the β chain of H2-A and H2-E molecules were not expressed differentially between CCR7^{-/-} and wild-type B cells. This finding was also verified by RT-PCR analysis (Fig. 1D). Together, these data suggest that only few genes are differentially expressed in B cells from CCR7^{-/-} mice and some of them have been associated with B-cell activation. Furthermore, the up-regulation of MHC-II observed on CCR7^{-/-} B cells is not caused by enhanced transcription of MHC-II genes in these cells.

analyzed only 12 were >2-fold over-expressed and 21 transcripts were >2-fold down-

MHC-II endocytosis rate is reduced in CCR7^{-/-} B cells

Since we could not find any difference in MHC-II expression at the mRNA level, we investigated the kinetics of MHC-II internalization and recycling by flow cytometry. Wild-type or CCR7^{-/-} B cells were labeled on ice with anti CD19-Cy5 and biotinylated anti-I-A^b, washed and then incubated for different time periods at 37°C. The cells were then

immediately washed on ice and the amount of MHC-II remaining on the cell surface was revealed with streptavidin-PerCp. MHC-II was internalized rapidly in CCR7^{+/+} as well as CCR7^{-/-} B cells. In both cell populations approximately 50% of the initial MHC-II amount remained on cell surface after 30 minutes while equilibrium was reached after 60 minutes (Fig. 2A). However, for all timepoints investigated, the rate of MHC-II endocytosis was significantly decreased in CCR7^{-/-} B cells (Fig. 2A). We also investigated the amount of MHC-II that recycled back to the cell surface from internal stores, or was newly translated, for the same time periods as described in the previous experiment. For this purpose B cells were labeled as described above and after incubation at 37°C were immediately washed on ice followed by staining with anti-I-A^b-FITC to reveal re-expressed MHC-II on the cell surface. The recycling kinetics of MHC-II to the cell surface were similar in CCR7^{+/+} and CCR7^{-/-} B cells (Fig. 2B). Together, these results suggest that the elevated expression of MHC-II on the cell surface of CCR7^{-/-} B cells is caused, at least to a certain extent, by a reduced MHC-II endocytosis rate.

CCR7^{-/-} B cells prime CD4⁺ T cells more efficiently than wild-type B cells

B cells can contribute as highly competent APCs to CD4⁺ T-cell activation [21, 22]. Thus we tested whether the altered activation phenotype of CCR7^{-/-} B cells is also associated with more efficient Ag presentation. The capacity of wild-type and CCR7^{-/-} B cells for Ag processing and presentation was assessed in vitro with a ³H-thymidine T-cell proliferation assay. Purified B cells from CCR7^{-/-} or wild-type mice were irradiated, incubated overnight with OVA₃₂₃₋₃₃₉-peptide or OVA protein and co-cultured with OT-II CD4⁺ T cells for three days. For all concentrations of OVA₃₂₃₋₃₃₉-peptide tested, CCR7^{-/-} B cells induced significantly higher CD4⁺ T-cell proliferation compared with CCR7^{+/+} B cells. While the increase in T-cell proliferation was on average approximately 2-fold in the case B-cells were pulsed with the peptide (Fig. 3A), an approximately 3-fold increase was observed for CCR7^{-/-} B cells loaded

with OVA protein (Fig. 3B). These observations suggest that the altered activation status of CCR7^{-/-} B cells, also is associated with very efficient Ag processing and presentation.

The altered cytokine milieu in pLNs of CCR7^{-/-} mice activates B cells

To address the question whether B cells in CCR7^{-/-} mice are activated due to a B-cell defect per se or due to the altered milieu present in pLNs in CCR7^{-/-} mice, we performed adoptive transfers of either CCR7^{-/-} or CCR7^{+/+} B cells in both wild-type and CCR7^{-/-} recipients. Ly5.1 donor B cells were transferred by i.v. injection to Ly5.2 wild-type and CCR7^{-/-} recipients. In the reverse experiment, TAMRA-labeled CCR7^{-/-} donor B cells were transferred to CCR7^{-/-} and wild-type recipients. 48 hours after cell transfer, the activation status of donor B cells in pLNs was measured by FACS. CCR7^{-/-} B cells that were introduced into the environment of wild-type pLNs significantly down-regulated their MHC-II expression, while CCR7^{+/+} B cells introduced into the environment of CCR7^{-/-} pLNs significantly up-regulated their MHC-II expression (Fig. 4A). These results suggest that B cells of CCR7^{-/-} mice do not carry an intrinsic defect that might account for their activated phenotype rather that the disturbed micromilieu of SLOs in CCR7^{-/-} mice constitutes a B-cell activating environment.

To test the possibility that an altered cytokine milieu in pLNs of CCR7^{-/-} mice is responsible for the activation of B cells, we performed RT-PCR analysis of transcripts for IL-4 and IFN-γ. Both prototypic cytokines that functionally define T_H2 or T_H1 immune responses, respectively, have been shown to modulate B cell functions [23]. In particular IL-4 has been described to efficiently activate B cells resulting amongst others in the up-regulated expression of MHC-II, CD23 and CD86 [23-25]. Total RNA from pLNs was reversely transcribed to cDNA and the expression of *Il4* and *Ifng* genes was assessed by RT-PCR. Of interest, IL-4 mRNA was approximately 23-fold enriched in pLNs of CCR7^{-/-} mice, while IFN-γ mRNA was expressed to a similar level in pLNs of CCR7^{-/-} and wild-type mice (Fig. 4B). Expression of both, IL-4 mRNA and IFN-γ mRNA was normalized to *hprt*

Immunology To substantiate the role of IL-4 in the B-cell activation observed in pLNs of CCR-/-

mice we performed in vivo IL-4 and/or IFN-γ neutralization assays. To this end CCR7^{-/-} mice were injected i.p. with either anti-IL-4 or anti- IFN-γ, or both neutralizing antibodies together. After 24h mice were sacrificed and MHC-II as well as CD86 surface expression levels of B cells in pLNs were assessed by flow cytometry. When compared with the negative control group injected with PBS we failed to observe any significant effect of IFN-γ blocking on MHC-II and CD86 expression. In contrast, anti-IL-4 mAb treatment led to a significant down-regulation of surface MHC-II and CD86 on B cells of CCR7^{-/-} mice (Fig. 4C). Furthermore, the combined application of anti IL-4 and anti IFN-γ neutralizing antibodies induced a similar impairment of B-cell activation as sole anti-IL-4 treatment. These data suggest that pLNs in CCR7^{-/-} mice harbor a T_H2 cytokine milieu characterized by abundant IL-4 expression and that this IL-4, but not IFN-γ, plays a significant role for the constitutive activation of B cells observed in pLNs of CCR7^{-/-} mice.

CCR7^{-/-} CD4⁺ T cells express higher levels of IL-4 in pLNs than wild-type CD4⁺ T cells

In order to assess the cellular source of IL-4 in pLNs of CCR7^{-/-} mice we investigated the IL-4 secretion potential of T cells. For this purpose single cell suspensions from pLNs of CCR7^{-/-} and wild-type mice were stimulated for 4 hours with PMA / ionomycin and IL-4 secretion from CD4⁺ T cells was determined on single cell level using the IL-4 secretion assay. We found approximately 4-times more IL-4-producing cells in pLNs of CCR7^{-/-} mice but no significant difference in IFN-γ expressing cells further substantiating the hypothesis that a

T_H2 environment is present in CCR7^{-/-} mice (Fig. 5A). There were no significant differences between wild-type and CCR7^{-/-} splenic CD4⁺ T cells regarding IL-4 secretion. However, cells in spleens of wild-type mice produced approximately 3-times more IFN-γ (Fig. 5B). Finally in order to test the hypothesis that absence of CCR7 on T cells affects their T_H2 polarization

Immuno

potential, we subjected naïve (CD62L⁺CD44⁻) CD4⁺ T cells sorted from LNs to T_H2 specific polarization *in vitro*. Cells were activated by anti-TCRβ, anti-CD28 and IL-2 under T_H2 conditions for 5 days. During the last 4 hours of culture cells were re-stimulated with PMA / ionomycin, and IL-4 expression of CD4⁺ T cells was assessed with the IL-4 secretion assay. Under these conditions approximately 5% of CCR7^{+/+} CD4⁺ T cells produced IL-4, whereas about 10% of CCR7^{-/-} CD4⁺ T cells were positive for secreted IL-4 (Fig. 5C). Together these data suggest that CCR7^{-/-} CD4⁺ T cells in pLNs are more prone to differentiate in the T_H2 direction than CCR7^{+/+} CD4⁺ T cells, contributing to the IL-4 rich environment in pLNs of CCR7^{-/-} mice.

3. Discussion

In addition to its role in cell homing, recent data suggest that CCR7 delivers signals that contribute to T-cell velocity [26], T-cell expansion as well as differentiation. CCL21, produced by LN stroma cells, but also present on the surface of DCs, delivers co-stimulatory signals during early TCR activation, leading to enhanced IFN-γ production and T_H1 polarization [12, 27]. Thus, active CCR7 signaling seems to favor T_H1 polarization of T cells. Our data support this idea, since absence of CCR7 signals skews the differentiation of T cells to the T_H2 direction. Compared with wild type controls, massively increased levels of IL-4 mRNA are found in LNs of CCR7^{-/-} mice and more IL-4 producing CD4⁺ T cells are present in the LNs of these animals. Apart from CD4⁺ T cells, approximately 0.15% of B cells secreted IL-4 in LNs of CCR7^{-/-} mice. In the CD8⁺ T cell population and the CD3⁻B220⁻ population no IL-4 secreting cells could be identified (data not shown). The increased levels of IL-4 probably contribute to the approximately 20-fold increase in serum IgE observed earlier in CCR7^{-/-} mice [6]. Using highly purified naïve CD4⁺ T cells in T_H2 polarization assays, our data suggest that the absence of CCR7 on CD4⁺ cells (and thus signals mediated via this receptor) directly contribute to T-helper-cell polarization since twice as many CCR7^{-/-} T cells gained a T_H2 phenotype compared with wild-type cells. However, since CCR7deficiency also affects the homing of several cell types into LNs we can not exclude additional factors contributing to the T_H2 environment in these mice. Furthermore, detection of IL-4 by standard methods such as intracellular staining or secretion assay reveals only a fraction of IL-4-producing T cells when compared with the detection of IL-4 transcription levels using IL4-reporter mice [28]. This discrepancy along with yet unknown factors might help to explain why IL-4 transcript levels were considerably higher than the number of IL-4producing T cells in CCR7^{-/-} mice. In particular, the impairment of CCR7^{-/-} DC to home to LNs following their activation in the periphery affects antigen presentation in these mice which also might have an effect on T-cell polarization. Furthermore, the positioning of those

T cells which successfully homed to LNs in CCR7^{-/-} mice is considerably different from the wild-type situation. While B and T cells, to a large degree, are separated in wild-type animals, these cells are not clearly segregated in CCR7^{-/-} animals, with large numbers of CD4⁺ T cells invading the B-cell follicles [29] (see also Fig. S3). This delocalization of T cells allows multiple interactions with B cells and potentially contributes to their activation in LNs of CCR7^{-/-} mice.

of interest, using *L. major* infection in IL-4 reporter (4-get) mice Reinhardt et al. [30] recently reported that not the classical T_H2 cells but rather T follicular helper (T_{FH}) cells are the main producers of IL-4 in vivo. Among others, T_{FH} cells are characterized by the expression of CD154, a potent B-cell activator, ICOS, PD-1, as well as expression of CXCR5 and absence of CCR7. Previous studies from our own group and others have shown that the localization of T_{FH} cells in SLOs is determined by the balanced expression of CCR7 and CXCR5 [29, 31]. While the lack of CXCR5, a receptor for CXCL13 produced by follicular dendritic cells, prevents migration of T_{FH} cells from the T-zone to B-cell follicles, the lack of CCR7 disrupts T-zone retention signals and allows translocation of all CXCR5⁺ cells to the follicle. IL-4 producing CD4⁺ T cells in pLNs of CCR7^{-/-} mice exhibit a similar localization pattern to T_{FH} cells and a significant proportion of these cells co-expresses the characteristic T_{FH} markers ICOS and PD-1 (Fig. S4). Thus it is plausible that not only a shifted T_H2 polarization but also displacement of activated T cells into the B-cell follicle are causative for the activated B cells found in LNs of CCR7^{-/-} mice.

Several signals are known to be required for efficient B-cell activation including Ag engagement of the BCR, ligation of CD40 by CD154, presence of DC, as well as IL-4 provided by activated CD4⁺ T cells and DCs [32, 33]. CD40 signaling sustains B-cell activation and leads to several modifications in the Ag processing and presentation machinery [34]. These changes include enhanced Ag processing, up-regulation of MHC-II and stabilization of CD86-expression [35]. Thus, the process of B-cell activation is highly

[6]. Applying adoptive B-cell transfers, we could demonstrate that CCR7-deficiency on B cells does not directly lead to the activation of these cells but that environmental factors within the pLNs of CCR7^{-/-} mice lead to B-cell activation. Using neutralizing antibodies, these experiments revealed IL-4 as a key component that leads to MHC-II and CD86 up-regulation on B cells. Several reports have addressed the role of IL-4 in B-cell activation. IL-4 leads to up-regulation of MHC-II, CD23 on B cells and induction of IgE production [23, 24, 36, 37]. Similar effects were observed in studies assessing the effects of IL-4 and IL-13 in human B cells [38-40]. IL-4 is not only a major B-cell activating factor that is effectively produced by helper CD4⁺ T cells but, through a positive feedback loop, it reinforces T_H2 polarization of CD4⁺ T cells [41] thus contributing to increase IL-4 in LNs of CCR7^{-/-} mice. Furthermore, as outlined above, CD4⁺ T cells in pLNs of CCR7^{-/-} mice are displaced to a large degree to the B cell follicle and, thus, it seems possible that B cells get not only activated via secreted IL-4 but also by CD40 signaling induced by membrane-bound CD154. Of interest, activated B cells have been reported to be able to elicit their own help from T cells and to induce T_H2 differentiation of CD4⁺T cells through efficient Ag presentation [42]. Since B cells in CCR7^{-/-} mice not only show an activated phenotype but also efficiently present Ag to CD4⁺ T cells, it seems possible that these cells provide a feedback loop that contributes to the extended T_H2 polarization in these animals. The strong T-cell priming capabilities of CCR7^{-/-} B cells can be probably attributed to the enhanced co-stimulation provided by the abundant CD86 expression and increased amounts of Ag presented in the elevated levels of surface MHC-II molecules. These properties likely account for the significantly higher T-cell proliferation observed. However we can currently not exclude that additional factors contribute to this effect.

dependent on interactions with T cells and DC, both being severely affected in CCR7^{-/-} mice

A number of reports assessed the role of CCR7 signaling in the induction of $T_{\rm H2}$ responses. Employing a well established model of OVA mediated allergic airway

inflammation, Xu et al. show that *plt/plt* mice develop a higher allergic inflammation score in the lung including significantly enhanced recruitment of eosinophils and lymphocytes compared with wild-type mice [43]. Furthermore, OVA-specific and total IgE levels were substantially higher in *plt/plt* mice as well as IL-4 and IL-13 expression levels in the lung when compared with wild-type mice. In contrast, compared with wild type animals the expression of IFN-γ was lower in *plt/plt* animals. Similar results were obtained in studies by Takamura et al. and Grinnan et al. [44, 45]. In summary, these studies provide evidence for enhanced T_H2 responses upon immunization in the absence of functional CCR7 signaling.

As it has been reported by Pai et al. [25], the IL-4-induced up-regulation of MHC-II protein expression on B cells is not due to enhanced transcription of MHC-II or CIITA, the

As it has been reported by Pai et al. [25], the IL-4-induced up-regulation of MHC-II protein expression on B cells is not due to enhanced transcription of MHC-II or CIITA, the master regulator of MHC-II expression. We obtained identical results from our microarray studies and qRT-PCR experiments comparing transcript expression in CCR7^{-/-} versus wild-type B cells. CIITA and H2 transcripts were not differentially expressed between both genotypes. Accordingly, posttranslational mechanisms have been speculated to be responsible for increased MHC-II expression induced by IL-4 in B cells. By addressing the kinetics of MHC-II internalization and recycling in CCR7^{-/-} B cells we present evidence that a reduced MHC-II endocytosis rate contributes to the up-regulation of MHC-II and by neutralizing IL-4 in vivo we provided substantial evidence for IL-4 significantly contributing to the activation of B cells in CCR7^{-/-} mice. Linking these two findings, we propose a model for an IL-4-mediated reduction of MHC-II endocytosis from the cell surface, at least contributing by as yet unknown mechanisms to the IL-4 mediated MHC-II up-regulation in B cells described here and by others [23, 25].

Taken together, our findings support the hypothesis that signaling through CCR7 affects the $T_H 1/T_H 2$ polarization potential of $CD4^+$ T cells with lack of CCR7 signaling favoring the development of $T_H 2$ cells. The increased IL-4 production potentially together with the delocalization of $CD4^+$ T cells into the B-cell follicle contributes to B-cell activation

in pLNs of CCR7^{-/-} mice. These activated B cells efficiently prime CD4⁺ T cells and thus

potentially contribute to the T_H2 microenvironment in CCR7^{-/-} mice.

4. Materials and Methods

Mice

BALB/c CCR7^{-/-} and C57BL/6 CCR7^{-/-} mice as well as BALB/c, C57BL/6, C57BL/6 Ly5.1, OT-II and C57BL/6 *plt/plt* mice were bred at the animal facility of Hannover Medical School. All mice were maintained under specific pathogen-free conditions and used at the age of 8-12 weeks. Animal experiments were conducted in accordance with local and institutional guidelines.

Antibodies and Flow cytometry

Single-cell suspensions from pLNs (pooled inguinal, axillary and brachial lymph nodes), spleen and peripheral blood were incubated for 20 min at 4 °C with fluorochrome-labeled antibodies in FACS staining buffer (PBS with 3% (vol/vol) FCS). Data were collected on a LSR II flow cytometer (BD Biosciences) and were analyzed with FlowJo software (Treestar). The following antibodies were used: anti-I-A^b-bio/FITC, anti-I-A^d-FITC and anti-CD3-PE (all from BD Biosciences); anti-CD23-PE (Caltag); anti-CD86-allophycocyanin, anti-CD45.1-PE, anti-CD62L-allophycocyanin-eFluor® 780, anti-CD44-eFluor® 450 and anti-CD45.2-PerCp Cy5.5 (eBioscience); and anti-CD4-PerCp (BioLegend). The following antibodies were grown at our institutes: anti-TCRβ chain-bio (clone: H57-597), anti-CD19-bio/Cy5 (clone 1D3), anti-IL-4 (clone 11B11), anti-IFN-γ (clone XMG1.2) and anti-B220-PO (clone TIB146). PerCp (BD Biosciences) or Pacific Orange (Invitrogen) -labeled streptavidin was used for detection of primary biotinylated antibodies. FMO (fluorescence-minus-one) or isotype control samples were used to assess background fluorescence for each population [46].

Adoptive cell transfers

Single-cell suspensions were prepared from spleens of C57BL/6 Ly5.1 and C57BL/6 CCR7^{-/-} donor mice. Cells from the latter were labeled with 7.5 μM 5-(and-6-) TAMRA SE (Invitrogen) for 15 min at 37 °C. C57BL/6 Ly5.2 and C57BL/6 CCR7^{-/-} mice received 15 x 10⁶ cells by i.v. injection into the tail vein. Recipient mice were sacrificed 48 hours after cell transfer.

T-cell proliferation assays

For T-cell proliferation assays, B cells from wild-type or CCR7 $^{-/-}$ mice were purified by positive selection using mouse CD45R (B220) MicroBeads and AutoMacs (Miltenyi Biotec) resulting routinely in > 95% purity of B cells. These cells were irradiated at 30 Gy and pulsed overnight with different concentrations of OVA peptide specific for the TCR expressed by OT-II T cells (OVA₃₂₃₋₃₃₉ ISQAVHAAHAEINEAGR; peptide. (Anaspec) or with 1 mg/ml OVA grade VI (Sigma-Aldrich). CD4 $^+$ T cells from OT-II mice were purified by magnetic sorting using mouse CD4 Dynabeads (Invitrogen) or mouse CD4 T Cell Isolation Kit and AutoMacs (Miltenyi Biotec). Cells were co-cultured in complete RPMI 1640 (10% FCS, β -ME, glutamine, penicillin/streptomycin) at a ratio of 1:1 for 72 h in triplicates, with 0.8 μ Ci 3 H-thymidine added for the last 18 h of culture. Proliferation of CD4 $^+$ T cells was determined with a scintillation counter.

T-cell polarization assays

Single-cell suspensions were prepared from lymph nodes or spleens of BALB/c CCR7^{-/-} and BALB/c mice. Cells were stimulated for four hours with 50 ng/mL phorbol myristate acetate (Sigma-Aldrich) and 500 ng/mL ionomycin (Invitrogen) in complete RPMI and subjected to the Mouse IL-4 Secretion Assay (Miltenyi Biotec) for detection of IL-4 production according to the instructions of the manufacturer. For intracellular IFN-γ staining, cells were stimulated for four hours with 50 ng/mL phorbol myristate acetate and 500 ng/mL ionomycin. During

the last two hours of culture 10 μ g/ml Brefeldin A (Sigma-Aldrich) was added. Cells were then fixed and permeabilized using the BD cytofix/cytoperm Kit (BD Biosciences).

Intracellular cytokine staining was performed using anti- IFN-γ-PE (Biolegend).

For T_H2 polarization assays naïve $CD4^+$ T cells from LNs were sorted on a FACSAria (BD Biosciences) after staining with anti-CD4, anti-CD62L and anti-CD44, to > 99% purity. Cells were stimulated in 96-well plates under T_H2 conditions as described before in the presence of antigen-presenting-cells prepared from spleens of BALB/c mice after γ -irradiation and T-cell depletion. In brief, cells were activated with anti-TCR β (1 μ g/ml, clone H57), anti-CD28 (5 μ g/ml, clone 37.51), human recombinant IL-2 (50 U/ml) and differentiated under T_H2 conditions with 40 ng/ml murine recombinant IL-4 (PeproTech), 10 μ g/ml anti IL-12 (clone C17.8) and 40 μ g/ml anti IFN- γ (clone XMG 1.2) [28]. Cells were cultured at a ratio of 1:3 (50 000 CD4 $^+$ T cells with 150 000 APCs) for 5 days. After 5 days in culture cells were restimulated with 50 ng/mL phorbol myristate acetate and 500 ng/mL ionomycin for 4 hours, and blocking of IL-4 bound to the IL-4R was performed with purified anti-IL-4 (clone BVD6-24G2), 100 μ g/ml. For detection of IL-4 secreting cells the mouse IL-4 Secretion Assay (Miltenyi Biotec) was used.

MHC-II internalization and recycling assay

Single cell suspensions from pooled pLNs of wild-type or CCR7^{-/-} mice were incubated with anti-CD19-APC and biotinylated anti-I-A^b (clone AF6-120.1) on ice. Cells were washed twice with ice-cold FACS Buffer. Some aliquots were then further incubated for various time periods ranging from 10 minutes to 2 hours in RPMI 1640 supplemented with 5% FCS at 37°C. The cells were then immediately washed twice in a 10-fold volume of ice-cold FACS buffer and stained on ice with Streptavidin-PerCP or with anti-I-A^b-FITC (clone AF6-120.1). The MFI of MHC-II was determined by flow cytometry.

Real-time PCR

Total RNA was extracted from pLNs that had been snap-frozen in 0.5 ml of TRIzol reagent (Invitrogen). Samples were thawed, homogenized using a QIAGEN TissueLyser II, and total RNA was extracted according to manufacturer's instructions. cDNA was then generated from individual RNA samples using Superscript II Reverse Transcriptase (Invitrogen) and random hexamer primers. The relative expression of the genes of interest was assessed using a LightCycler 2.0 (Roche) and SYBR Premix Ex Taq kit (Takara Bio Inc.). cDNA samples were assayed in duplicate. The cycle threshold was used for quantification. Gene expression levels for each individual sample were normalized to HPRT. Relative gene expression (fold change) between samples was calculated using the mathematic model described by Pfaffl [47]. The following primers were used:

IL4 (forward), CATCGGCATTTTGAACGAG;

IL4 (reverse), CGAGCTCACTCTGTGGTG;

 $IFN-\gamma \ (forward), \ ATCTGGAGGAACTGGCAAAA;$

IFN-γ (reverse), TTCAAGACTTCAAAGAGTCTGAGGTA;

H2-Ab1 (forward), GTGGTGCTGATGGTGCTG;

H2-Ab1 (reverse), CCATGAACTGGTACACGAAATG;

H2-Eb1 (forward), CCGTTGTAGAAATGACACTCAGA;

H2-Eb1 (reverse), CCTCCAGTGGCTTTGGTC;

HPRT (forward), TCCTCCTCAGACCGCTTTT;

HPRT (reverse), CCTGGTTCATCATCGCTAATC;

Primer pairs were designed with Universal Probe Library website (Roche).

Microarray experiments

In two independent experiments, B cells from peripheral lymph nodes of three C57Bl/6 - CCR7^{-/-} and three wild-type mice were sorted on a FACSAria (BD Biosciences) and subjected

Immuno

to total RNA isolation (Nucleospin RNA XS kit, Macherey & Nagel). Samples from all individuals of the same genotype were pooled (using 9 ng of RNA per individual). The Whole Mouse Genome Oligo Microarray 4x44K (G4122F, design ID 014868, Agilent Technologies) was utilized in this study. 20 ng of pooled total RNA per condition were used to prepare Cy3-, or Cy5-labeled cRNA (Amino Allyl MessageAmpTM II Kit; Ambion) according to manufacturer's instructions. Microarrays were co-hybridized with differently-labeled material from CCR7^{-/-} versus wild-type animals in a dual-color setting. Two biological replicate experiments were analyzed by use of two individual microarrays including a dye-swap.

Additional information on methodology and experimental design have been deposited along with complete microarray data in NCBI's Gene Expression Omnibus and are accessible through GEO Series accession number GSE27885

(http://www.ncbi.nlm.nih.gov/geo/query/acc.cgi?acc=GSE27885).

Statistical analysis

Statistical analyses were performed with GraphPadPrism 4 software. Unpaired two-tailed t tests were used to determine any significant differences between sample groups. Bars show mean values, error bars represent SD or SEM.

Immuno

Acknowledgement

We thank Andreas Krueger and Günter Bernhardt for fruitful discussions and critical comments on the manuscript. This work was supported by a Deutsche Forschungsgemeinschafts grant KFO 250 -FO 334/2-1, to R.F.

Disclosure of Conflicts of Interest:

The authors declare no financial or commercial conflict of interest

Ngo, V. N., Tang, H. L. and Cyster, J. G., Epstein-Barr virus-induced molecule 1 ligand chemokine is expressed by dendritic cells in lymphoid tissues and strongly attracts naive T cells and activated B cells. *J Exp Med* 1998. **188**: 181-191.

Sallusto, F., Lenig, D., Forster, R., Lipp, M. and Lanzavecchia, A., Two subsets of memory T lymphocytes with distinct homing potentials and effector functions. *Nature* 1999. **401**: 708-712.

Sanchez-Sanchez, N., Riol-Blanco, L. and Rodriguez-Fernandez, J. L., The multiple personalities of the chemokine receptor CCR7 in dendritic cells. *J Immunol* 2006. **176**: 5153-5159.

Seth, S., Oberdorfer, L., Hyde, R., Hoff, K., Thies, V., Worbs, T., Schmitz, S. and Forster, R., CCR7 essentially contributes to the homing of plasmacytoid dendritic cells to lymph nodes under steady-state as well as inflammatory conditions. *J Immunol* 2011. **186**: 3364-3372.

Forster, R., Davalos-Misslitz, A. C. and Rot, A., CCR7 and its ligands: balancing immunity and tolerance. *Nat Rev Immunol* 2008. **8**: 362-371.

Forster, R., Schubel, A., Breitfeld, D., Kremmer, E., Renner-Muller, I., Wolf, E. and Lipp, M., CCR7 coordinates the primary immune response by establishing functional microenvironments in secondary lymphoid organs. *Cell* 1999. **99**: 23-33.

Schneider, M. A., Meingassner, J. G., Lipp, M., Moore, H. D. and Rot, A., CCR7 is required for the in vivo function of CD4+ CD25+ regulatory T cells. *J Exp Med* 2007. **204**: 735-745.

Scandella, E., Fink, K., Junt, T., Senn, B. M., Lattmann, E., Forster, R., Hengartner, H. and Ludewig, B., Dendritic cell-independent B cell activation during acute virus infection: a role for early CCR7-driven B-T helper cell collaboration. *J Immunol* 2007. **178**: 1468-1476.

Davalos-Misslitz, A. C., Rieckenberg, J., Willenzon, S., Worbs, T., Kremmer, E., Bernhardt, G. and Forster, R., Generalized multi-organ autoimmunity in CCR7-deficient mice. *Eur J Immunol* 2007. **37**: 613-622.

Ziegler, E., Oberbarnscheidt, M., Bulfone-Paus, S., Forster, R., Kunzendorf, U. and Krautwald, S., CCR7 signaling inhibits T cell proliferation. *J Immunol* 2007. **179**: 6485-6493.

11

Immuno

Davalos-Misslitz, A. C., Worbs, T., Willenzon, S., Bernhardt, G. and Forster, R., Impaired responsiveness to T-cell receptor stimulation and defective negative selection of thymocytes in CCR7-deficient mice. *Blood* 2007. **110**: 4351-4359.

Gollmer, K., Asperti-Boursin, F., Tanaka, Y., Okkenhaug, K., Vanhaesebroeck, B., Peterson, J. R., Fukui, Y., Donnadieu, E. and Stein, J. V., CCL21 mediates CD4+ T-cell costimulation via a DOCK2/Rac-dependent pathway. *Blood* 2009. **114**: 580-588.

Mori, S., Nakano, H., Aritomi, K., Wang, C. R., Gunn, M. D. and Kakiuchi, T., Mice lacking expression of the chemokines CCL21-ser and CCL19 (plt mice) demonstrate delayed but enhanced T cell immune responses. *J Exp Med* 2001. **193**: 207-218.

Kashiwada, M., Levy, D. M., McKeag, L., Murray, K., Schroder, A. J., Canfield, S. M., Traver, G. and Rothman, P. B., IL-4-induced transcription factor NFIL3/E4BP4 controls IgE class switching. *Proc Natl Acad Sci U S A* 2010. **107**: 821-826.

Mather, E. L., Alt, F. W., Bothwell, A. L., Baltimore, D. and Koshland, M. E., Expression of J chain RNA in cell lines representing different stages of B lymphocyte differentiation. *Cell* 1981. **23**: 369-378.

Muramatsu, M., Kinoshita, K., Fagarasan, S., Yamada, S., Shinkai, Y. and Honjo, T., Class switch recombination and hypermutation require activation-induced cytidine deaminase (AID), a potential RNA editing enzyme. *Cell* 2000. **102**: 553-563.

Nakamura, A., Mori, Y., Hagiwara, K., Suzuki, T., Sakakibara, T., Kikuchi, T., Igarashi, T., Ebina, M., Abe, T., Miyazaki, J., Takai, T. and Nukiwa, T., Increased susceptibility to LPS-induced endotoxin shock in secretory leukoprotease inhibitor (SLPI)-deficient mice. *J Exp Med* 2003. **197**: 669-674.

Zhu, Y. X., Benn, S., Li, Z. H., Wei, E., Masih-Khan, E., Trieu, Y., Bali, M., McGlade, C. J., Claudio, J. O. and Stewart, A. K., The SH3-SAM adaptor HACS1 is up-regulated in B cell activation signaling cascades. *J Exp Med* 2004. **200**: 737-747.

Klaewsongkram, J., Yang, Y., Golech, S., Katz, J., Kaestner, K. H. and Weng, N. P., Kruppel-like factor 4 regulates B cell number and activation-induced B cell proliferation. *J Immunol* 2007. **179**: 4679-4684.

Reif, K. and Cyster, J. G., RGS molecule expression in murine B lymphocytes and ability to down-regulate chemotaxis to lymphoid chemokines. *J Immunol* 2000. **164**: 4720-4729.

- **Constant, S. L.,** B lymphocytes as antigen-presenting cells for CD4+ T cell priming in vivo. *J Immunol* 1999. **162**: 5695-5703.
- **Morris, S. C., Lees, A. and Finkelman, F. D.,** In vivo activation of naive T cells by antigen-presenting B cells. *J Immunol* 1994. **152**: 3777-3785.
 - Coffman, R. L., Seymour, B. W., Lebman, D. A., Hiraki, D. D., Christiansen, J. A., Shrader, B., Cherwinski, H. M., Savelkoul, H. F., Finkelman, F. D., Bond, M. W. and et al., The role of helper T cell products in mouse B cell differentiation and isotype regulation. *Immunol Rev* 1988. **102**: 5-28.
 - Keegan, A. D., Snapper, C. M., Van Dusen, R., Paul, W. E. and Conrad, D. H., Superinduction of the murine B cell Fc epsilon RII by T helper cell clones. Role of IL-4. *J Immunol* 1989. **142**: 3868-3874.
 - **Pai, R. K., Askew, D., Boom, W. H. and Harding, C. V.,** Regulation of class II MHC expression in APCs: roles of types I, III, and IV class II transactivator. *J Immunol* 2002. **169**: 1326-1333.
 - **Worbs, T. and Forster, R.,** T cell migration dynamics within lymph nodes during steady state: an overview of extracellular and intracellular factors influencing the basal intranodal T cell motility. *Curr Top Microbiol Immunol* 2009. **334**: 71-105.
 - **Flanagan, K., Moroziewicz, D., Kwak, H., Horig, H. and Kaufman, H. L.,** The lymphoid chemokine CCL21 costimulates naive T cell expansion and Th1 polarization of non-regulatory CD4+ T cells. *Cell Immunol* 2004. **231**: 75-84.
 - **Mohrs, M., Shinkai, K., Mohrs, K. and Locksley, R. M.,** Analysis of type 2 immunity in vivo with a bicistronic IL-4 reporter. *Immunity* 2001. **15**: 303-311.
 - **Hardtke, S., Ohl, L. and Forster, R.,** Balanced expression of CXCR5 and CCR7 on follicular T helper cells determines their transient positioning to lymph node follicles and is essential for efficient B-cell help. *Blood* 2005. **106**: 1924-1931.
 - **Reinhardt, R. L., Liang, H. E. and Locksley, R. M.,** Cytokine-secreting follicular T cells shape the antibody repertoire. *Nat Immunol* 2009. **10**: 385-393.
 - Ansel, K. M., Ngo, V. N., Hyman, P. L., Luther, S. A., Forster, R., Sedgwick, J. D., Browning, J. L., Lipp, M. and Cyster, J. G., A chemokine-driven positive feedback loop organizes lymphoid follicles. *Nature* 2000. **406**: 309-314.
 - **DeFranco, A. L.,** B-cell activation 2000. *Immunol Rev* 2000. **176**: 5-9.

33

Immuno

Wykes, M. and MacPherson, G., Dendritic cell-B-cell interaction: dendritic cells provide B cells with CD40-independent proliferation signals and CD40-dependent survival signals. *Immunology* 2000. **100**: 1-3.

Mills, D. M. and Cambier, J. C., B lymphocyte activation during cognate interactions with CD4+ T lymphocytes: molecular dynamics and immunologic consequences. *Semin Immunol* 2003. **15**: 325-329.

Rodriguez-Pinto, D., B cells as antigen presenting cells. *Cell Immunol* 2005. **238**: 67-75.

Conrad, D. H., Keegan, A. D., Kalli, K. R., Van Dusen, R., Rao, M. and Levine, A. D., Superinduction of low affinity IgE receptors on murine B lymphocytes by lipopolysaccharide and IL-4. *J Immunol* 1988. **141**: 1091-1097.

Kuhn, R., Rajewsky, K. and Muller, W., Generation and analysis of interleukin-4 deficient mice. *Science* 1991. **254**: 707-710.

Defrance, T., Carayon, P., Billian, G., Guillemot, J. C., Minty, A., Caput, D. and Ferrara, P., Interleukin 13 is a B cell stimulating factor. *J Exp Med* 1994. **179**: 135-143.

Ikizawa, K., Kajiwara, K., Koshio, T., Matsuura, N. and Yanagihara, Y., Inhibition of IL-4 receptor up-regulation on B cells by antisense oligodeoxynucleotide suppresses IL-4-induced human IgE production. *Clin Exp Immunol* 1995. **100**: 383-389.

Defrance, T., Aubry, J. P., Rousset, F., Vanbervliet, B., Bonnefoy, J. Y., Arai, N., Takebe, Y., Yokota, T., Lee, F., Arai, K. and et al., Human recombinant interleukin 4 induces Fc epsilon receptors (CD23) on normal human B lymphocytes. *J Exp Med* 1987. **165**: 1459-1467.

Zhu, J., Transcriptional regulation of Th2 cell differentiation. *Immunol Cell Biol* 2010. **88**: 244-249.

Stockinger, B., Zal, T., Zal, A. and Gray, D., B cells solicit their own help from T cells. *J Exp Med* 1996. **183**: 891-899.

Xu, B., Aoyama, K., Kusumoto, M., Matsuzawa, A., Butcher, E. C., Michie, S. A., Matsuyama, T. and Takeuchi, T., Lack of lymphoid chemokines CCL19 and CCL21 enhances allergic airway inflammation in mice. *Int Immunol* 2007. **19**: 775-784.

44

immuno

Grinnan, D., Sung, S. S., Dougherty, J. A., Knowles, A. R., Allen, M. B., Rose, C. E., 3rd, Nakano, H., Gunn, M. D., Fu, S. M. and Rose, C. E., Jr., Enhanced allergen-induced airway inflammation in paucity of lymph node T cell (plt) mutant mice. *J Allergy Clin Immunol* 2006. **118**: 1234-1241.

Takamura, K., Fukuyama, S., Nagatake, T., Kim, D. Y., Kawamura, A., Kawauchi, H. and Kiyono, H., Regulatory role of lymphoid chemokine CCL19 and CCL21 in the control of allergic rhinitis. *J Immunol* 2007. **179**: 5897-5906.

Roederer, M., Spectral compensation for flow cytometry: visualization artifacts, limitations, and caveats. *Cytometry* 2001. **45**: 194-205.

Pfaffl, M. W., A new mathematical model for relative quantification in real-time RT-PCR. *Nucleic Acids Res* 2001. **29**: e45.

Figure legends

Fig. 1. B cells are activated in the pLNs of CCR7^{-/-} mice. (A) Flow cytometry plots show expression of MHC-II, CD86 and CD23 on CD19⁺ cells from pLNs, spleen and peripheral blood in BALB/c (solid line) and BALB/c-CCR7^{-/-} mice (dashed line). Fluorescence minus one (FMO) controls for both genotypes are shown in gray-shaded histograms. (B)

Quantitation of results shown in (A). Data are presented as mean ± SD of three mice per group. Representative results are shown from one of three to five independent experiments.

(C) CD19⁺ cells were sorted from pLNs of CCR7^{-/-} and wild type mice and subjected to microarray analysis as described in Materials and Methods. The x-axis depicts log₂ transformed values of relative gene expression levels in CCR7^{-/-} B cells versus wild-type B cells. X-axis labels were re-converted to fold change values. Only genes with an established role in B-cell activation processes were selected for presentation. Bars represent mean and dots represent range of ratio values calculated from two individual experiments. (D) Uniform transcript expression of MHC-II genes in B cells isolated from pLNs of wild-type and CCR7^{-/-} mice. Relative expression of MHC-II genes was determined with RT-PCR. Data are presented as the mean and range of ratio values from three independent experiments.

Fig. 2. Reduced rate of MHC-II endocytosis in CCR7^{-/-} **B cells.** (A) Single cell suspensions generated from pLNs of CCR7^{-/-} and wild-type mice were stained on ice with anti-CD19 to identify B cells and biotinylated anti-I-A^b. The cells were then washed and incubated at 37°C for different periods of time as indicated. After incubation, cells were immediately washed extensively on ice and stained with a fluorescently labeled streptavidin to reveal the remaining amount of MHC-II molecules on the cell surface, or as depicted in (B), with anti-I-A^b, recognizing the same epitope as the biotinylated anti-I-A^b used in the initial staining, to reveal MHC-II molecules recycling to the cell surface. The MFI of MHC-II on B cells was measured by flow cytometry and is expressed as a percentage of the MHC-II MFI on the

surface of B cells that were not incubated at 37°C. For direct comparison of MHC-II modulation MFI values of non-incubated wild type (filled circles) and CCR7^{-/-} B cells (open circles) were each set to 100%. Data are presented as mean \pm SD of four mice per group. Results are shown from one of three independent experiments. *p<0.05, **p<0.01, unpaired two-tailed *t*-test.

Fig. 3. CCR7^{-/-} B cells prime CD4⁺ T cells very efficiently. (A) MACS-purified B cells from CCR7^{-/-} (open bars) and wild-type mice (filled bars) were irradiated, pulsed overnight with different concentrations of OVA₃₂₃₋₃₃₉ peptide and used as stimulators for CD4⁺ T cells isolated from OT-II mice. The T-cell/B-cell ratio was 1:1. T-cell proliferation was assessed after 3 days of co-culture in a 3 H-thymidine incorporation assay. (B) Same experimental procedure as that described in (A), but using 1 mg/ml OVA protein as Ag. Data are presented as mean \pm SD of quadruplicate cultures. Representative results are shown from one of three (A) or two (B) independent experiments. Statistical significance was determined by the unpaired two-tailed *t*-test.

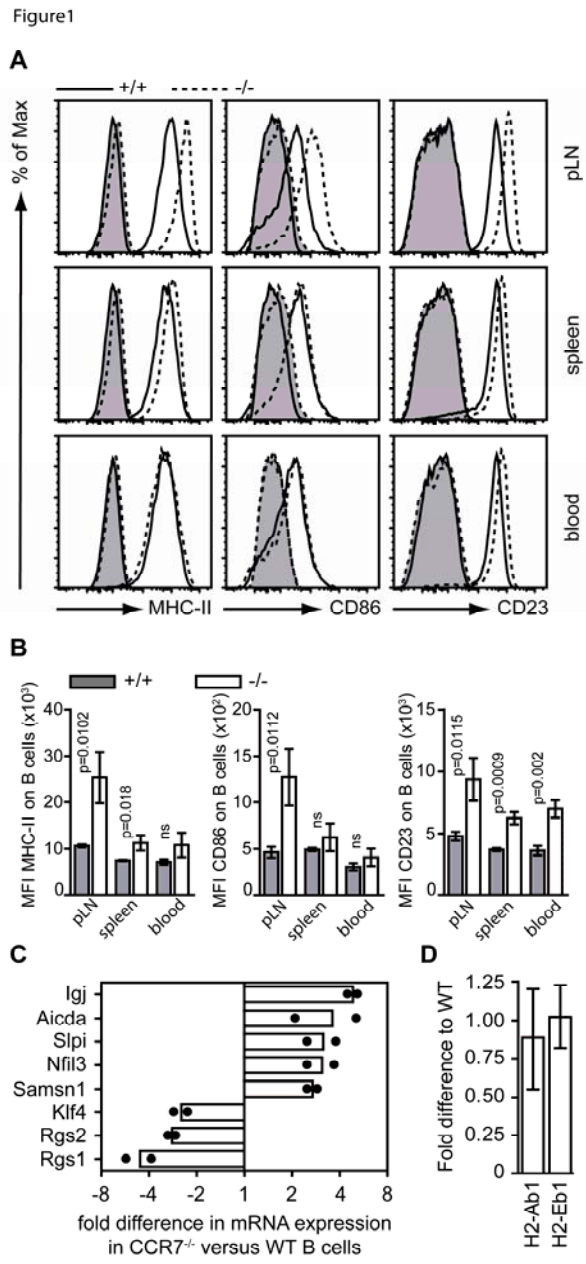
Fig. 4. The pLNs of CCR7^{-/-} mice exhibit a T_H2 cytokine milieu. (A) Single cell suspensions of TAMRA-labeled splenocytes from C57BL/6 CCR7^{-/-} or splenocytes from C57BL/6 Ly5.1 donor mice were adoptively transferred by i.v. injection in WT or CCR7^{-/-} recipients (recip.) as indicated. Recipients were sacrificed 48 hours after transfer and MHC-II surface expression on donor B cells in pLNs was analysed by flow cytometry (mean ± SD of four mice per group. Representative results from one of three independent experiments are shown. (B) Homogenized tissue samples of pLNs from CCR7^{-/-} and wild-type mice were assayed with RT-PCR for IL-4 and IFN-γ gene expression. The y axis shows relative expression levels in CCR7^{-/-} versus wild-type samples (mean ± SEM; n = 3 independent experiments). (C) CCR7^{-/-} mice were injected i.p. with either 0.9 mg of anti-IL-4 or 0.6 mg of

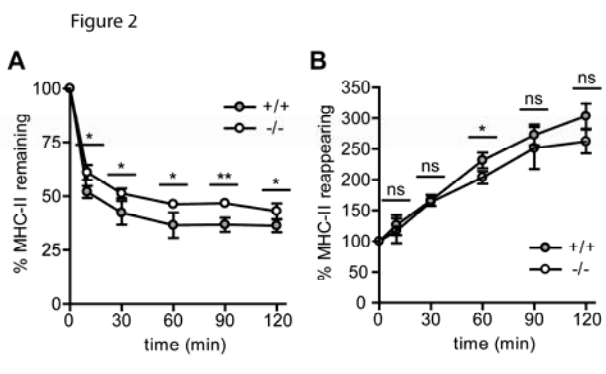
Immuno

anti-IFN- γ , or both antibodies. 24 hours after injection, mice were sacrificed and MHC-II (left) as well as CD86 expression (right) on B cells from pLNs was measured by flow cytometry. MFI values are plotted as a percentage of values obtained from CCR7^{-/-} mice injected with PBS, serving as control. Data are presented as mean \pm SEM of six mice per group. Results are shown from three pooled independent experiments. (A, C) Statistical significance was determined by the unpaired two-tailed *t*-test.

Fig. 5. CCR7^{-/-} CD4⁺ T cells in pLNs exhibit a high intrinsic T_H2 polarization potential.

(A) Single cell suspensions from pLNs of wild-type and CCR $7^{-/-}$ mice were stimulated for 4 hours with PMA / Ionomycin in complete RPMI. IL-4 secretion by CD4⁺ T cells was determined with the IL-4 secretion assay. For detection of IFN- γ production brefeldin A was added for the last 2 hours of culture and IFN- γ -expressing cells were identified by intracellular staining. (B) The same analyses were performed for cells isolated from spleens of wild-type and CCR $7^{-/-}$ mice. Representative flow cytometry plots and quantitation of data are shown from one of two independent experiments (4 mice per group). Numbers in gates present percent of CD4⁺ cells expressing IL-4 or IFN- γ . (C) Naïve CD4⁺ T cells were FACS-sorted from LNs and cultured under TH2 conditions for 5 days. After restimulation with PMA / Ionomycin cells were subjected to the IL-4 secretion assay and IL-4 production was measured by flow cytometry. Representative plots and quantitation of data (right) are shown from three pooled independent experiments. Data are presented as mean \pm SD of triplicate cultures per experiment. Statistical significance was determined by the unpaired two-tailed t-





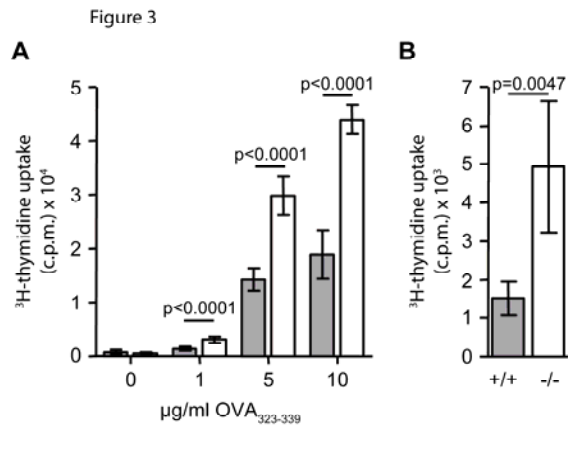
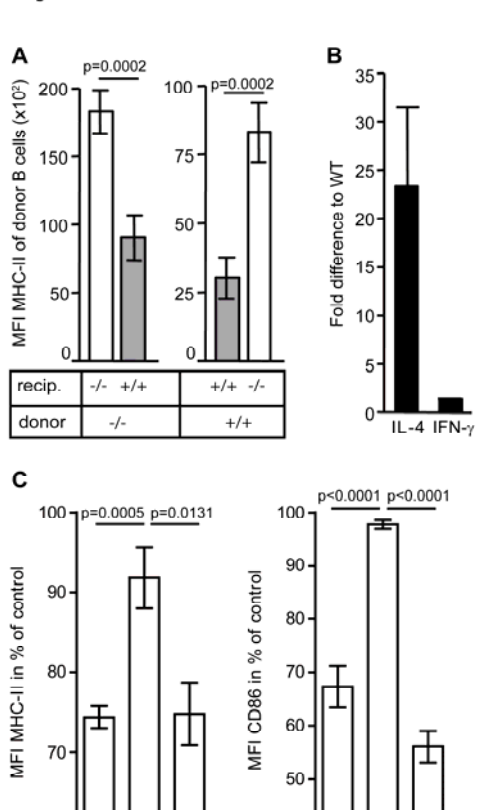


Figure 4

α-IL-4 α-IFN-γ

 α -IL-4 + α -IFN- γ



α-IL-4 α-IFN-γ α -IL-4 + α -IFN- γ

